Vol. (1), No (2), April-June 2024 DOI:10.21608/MERMJ.2024.272097.1012

Influence of heat treatment of optical properties on $Nd_{0.7}Ca_{0.3}MnO_3$ prepared by solid state reaction

Ibrahim Y. Khaled[*1].
1. Department of Basic Science, Faculty of Physiotherapy, Merit University.
* Corresponding author.

ARTICLEINFO

Article history:
Received 6 July 2024
Accepted 31 July 2024
Available online 26 November 2024

Keywords:
Perovskite's, Optical Properties, Refractive Index, and Manganite's.

Abstract

Annealed $Nd_{0.7}Ca_{0.3}MnO_3$ samples (untreated, 700ºC, 800ºC and 900ºC) were investigated by solid state reaction method. Studies happened into the variations in the optical parameters of NCMO samples were calculated from measurements of reflectance obtained with a spectrophotometer. Studies occurred on the associations between photon energy and absorption coefficient. The study showed that the optical transition is indirectly transition. The highest energy gap for as prepared NCMO is about 4.2 eV which makes the compound used as a absorber of the solar system applications.

Introduction

Research on rare earth manganite and perovskites with the overall formula $A_{1-x}B_xMnO_3$, where B is an alkaline earth divalent ion, such as Ca^{+2}, Sr^{+2}, or Ba^{+2}, and A is a trivalent rare earth ion like La^{+3}, Nd^{+3}, Pr^{+3}, etc., have been the subject of intense material science research recently because of their many technological uses [1-4]. In these materials, magnetic and electronic phases can coexist or be in competition. One of the interesting characteristics of manganite is seen in the charge ordering (CO) phase. It is an insulating phase that is unstable to various perturbations, such as electric, magnetic, and pressure fields. It has been shown [5-8] that, even at the Nano scale, it is unstable. Present manganite research focuses on how these materials' physical properties are affected by particle size reduction [9, 10]. Because surface disorder has an impact, particles with smaller grains have more varied magnetic and electrical characteristics. Publicly available studies on nano-manganite's provide fascinating results on the size decrease in these systems. In addition to the d-d interactions of manganese ions, the f-d and f-f interactions of rare-earth ions also influence the magnetic characteristics of another rare-earth manganite. At low temperatures, their contribution to the magnetic state is comparable to that of a manganese B-sublattice.

The remarkably unique magnetic characteristics of the $Nd_{1-x}Ca_xMnO_3$ family set it apart from other low-doped rare-earth manganite at low temperatures [11]. The interactions between the magnetically active Nd- and Mn- sublattices in this system show notable irregularities in the magnetization behavior. Analysis of the magnetic characteristics of the $Nd_{1-x}Ca_xMnO_3$ system can provide quick insights into the process of the antiferromagnet-ferromagnet phase transition in low-temperature and Nd-Mn magnetic coupling because of the significant fluctuations in the hole-doping level. Both charge ordering (CO) and orbital ordering (OO) are present in some manganite. Both a jump in resistivity and a structural phase change are expected on charge ordering. In fact, there have been a few investigations on charge ordering and field-induced structural phase transitions.

The octahedral network buckles when doped with the smaller rare earth ion Nd^{+3}, which results in a larger displacement of the crystal structure. This modifies bond angles and lengths, which affects double exchange (DE) interaction and electron hopping. The published papers on nano manganite's show the exciting implications of the size decrease in these systems, but many of the results are contradictory. We studied the $Nd_{0.7}Ca_{0.3}MnO_3$ nano-manganite in order to better understand the effects of annealing temperature and reduction size on the optical characteristics and dielectrics of manganates.

Materials and methods

As previously reported [12], ($Nd_{0.7}Ca_{0.3}MnO_3$) composites were produced through the traditional solid-state reaction technique. The optical properties were measured using a Jasco V-570 twin beam UV-visible-NIR spectrometer, which has a wavelength range of 400 to 2500 nm at normal incidence with a photometric accuracy of 0.31% transmittance and 0.0021-0.0042 absorbance [13]. The dielectric properties were examined using Hioki IM3536 type LCR meters [14].

Results & discussion

Structural properties

All of the annealed samples, as reported in Ref. [12], exhibit a single orthorhombic crystal structure phase that belongs to the Pbnm space group in $Nd_{0.7}Ca_{0.3}MnO_3$ and are free of any impurity peaks, based on the X-ray and Rietveld refinement techniques. The as-prepared NCMO has a smooth surface, more grain agglomerates when the annealing temperature rises, and more of them collide with one another, according to SEM images. Grain size and crystallites show a tendency to grow as the annealing temperature rises.

Investigation of the optical properties

The optical characteristics of the synthesized Nano composite in the UV and visible regions of the electromagnetic spectrum are examined using an ultraviolet-visible spectrophotometer. By employing the Kubelka-Munk function model, the bandgap is measured [13].

$$F(R) = \alpha = \frac{(1-R)^2}{2R} \qquad (1)$$

F(R) is the Kubelka-Munk function, where $\mathbf{F(R) = \alpha h\nu}$, α is absorbance coefficient and R is Reflectance value.

$$\alpha h\nu = A(h\nu - E_g)^{\,n} \qquad (2)$$

where the indirect and the direct and indirect transitions provided by n=2 and n=1/2, respectively. Using the Tauc plot of linear extrapolation between $[F(R)h\nu]^{1/2}$ and $h\nu$, the indirect bandgap value is computed. The following relations were also used to compute the optical dielectric constant's real (ε_r) and imaginary (ε_i) components, the refractive index (n), the extinction coefficient (k), the dissipation factor (tanδ), and the optical conductivity (σ_{opt}) at various wavelengths (λ)[14].

$$k = \frac{\propto \lambda}{2\pi} \qquad (3)$$

$$n = \frac{1+R}{1-R} + \sqrt{\frac{4R}{(1-R)^2}k^2} \qquad (4)$$

$$\varepsilon_r = n^2 - k^2 \qquad (5)$$

$$\varepsilon_i = 2nk \qquad (6)$$

$$\tan(\delta) = \frac{\varepsilon_r}{\varepsilon_i} \qquad (7)$$

$$\sigma = \frac{\alpha n c}{4\pi} \qquad (8)$$

In space, light travels at the speed of c. The amount that light travels through a substance at a slower speed than in vacuum is determined by its refractive index, or n. The refractive index dependency on wavelength at various annealing temperatures and green states is shown in Fig. 1. The refractive index values of the various samples at a wavelength of 650 nm are 1.17, 1.17, 1.17, 1.18, and 1.17 for the unheated, 700, 800, and 900 annealed samples of $Nd_{0.7}Ca_{0.3}MnO_3$, respectively. where there was a little change in refractive after it originally increased. Variations in material densities, surface defects, anisotropy, etc. could all be contributing factors to the refractive index shift between samples.

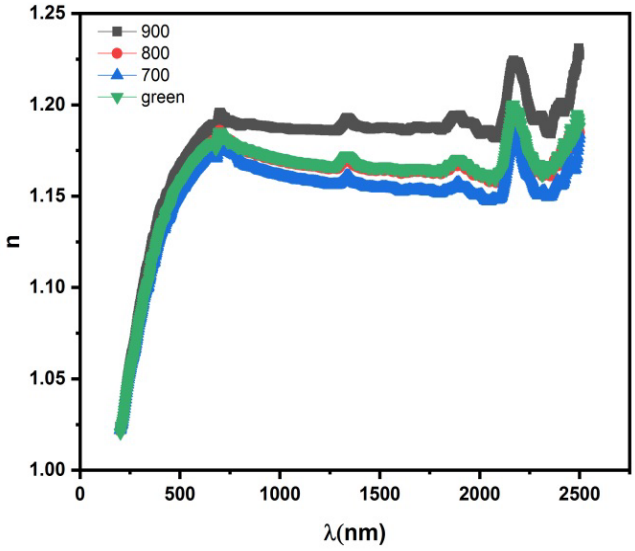

Fig. 1 shows the refractive index's fluctuation with wavelength

Figure 2 shows the relationship between hν and $(\alpha h\nu)^{1/2}$. The value of the indirect optical band gaps, or E_g, is obtained by projecting the linear part of the curve onto the energy axis and finding the intercept in this connection. The obtained E_g values for (Unheated, 700, 800, 900) K are (4.219, 3.883, 3.929, 4.128 eV). The energy band gap in the green sample is highest at T_{an} = 700 K, lowest at T_{an} = 800 K, then increases once more at T_{an} = 900 K. With higher annealing temperatures, there is a decrease in optical band gaps, which could be associated with a higher likelihood of poor crystallinity $Nd_{0.7}Ca_{0.3}MnO_3$ formation and therefore more defects in the samples. Furthermore, the optical band gaps grow as the annealing temperature rises, possibly due to the temperature's effect on the pinholes, which decreases as the temperature rises. These samples are a potential option for use as absorbers in solar cell system applications due to their E_g values.

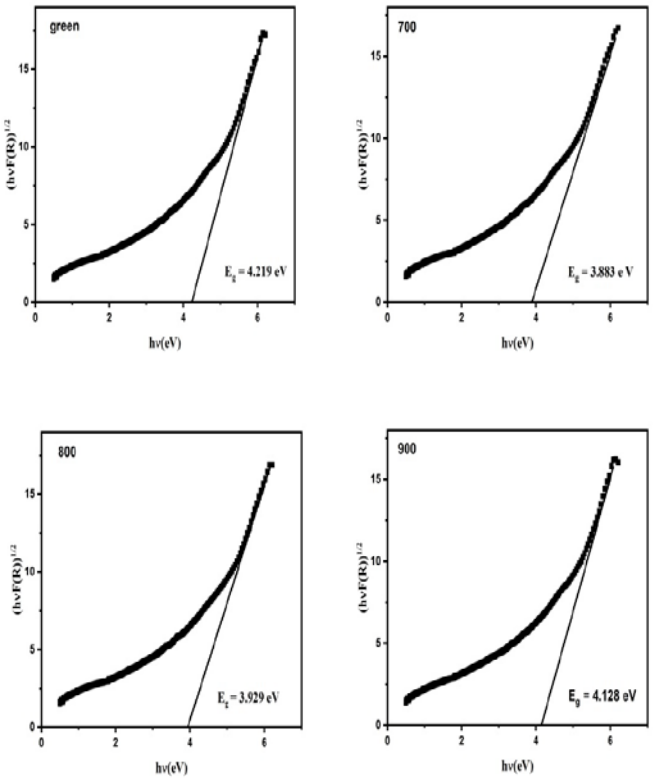

Fig. 2 Schematics of $(F(R)h\upsilon)^{1/2}$ vs hυ for as prepared $Nd_{0.7}Ca_{0.3}MnO_3$ and annealed samples.

The dielectric constant not only indicated the value of any fixed ionic charges in the lattice but also the degree to which an object's electric field is attenuated in comparison to vacuum. Fig. 3 shows how the dissipation factor and real and imaginary components of the dielectric constant vary with wavelength for all samples.

The true dielectric constant values for unheated, 700, 800, and 900°C are 1.33, 1.32, 1.33, and 1.36, respectively, as can be seen in Figure 3 at a wavelength of 500 nm. The real component of the dielectric constant increases exponentially for all samples at low wavelengths until it reaches (λ=650 nm), at which point it fluctuates. For (Unheated, 700, 800, and 900°C, the real part of the dielectric constant values is 1.38, 1.37, 1.38, and 1.41, respectively. The true part's value grows with temperature, and this is influenced by the annealing temperatures. Conversely, the dissipation factor and imaginary part values rise linearly after initially decreasing to (λ=390 nm). It has values at (λ=390 nm) equal to (1.03×10^{-6}, 1.05×10^{-6}, 1.01×10^{-5}, 9.46×10^{-6}) for unheated, 700, 800, 900°C respectively, and the annealing temperature promote the value of the imaginary part except at (T_{an} = 900°C). Higher dielectric constants indicated improved screen-charge screening abilities, which may result from ionic or electronic contribution [15]. Moreover, a high dielectric constant reduces the potential barrier and spatial extent of a charged defect, which lessens the propensity for free carriers to scatter [16].

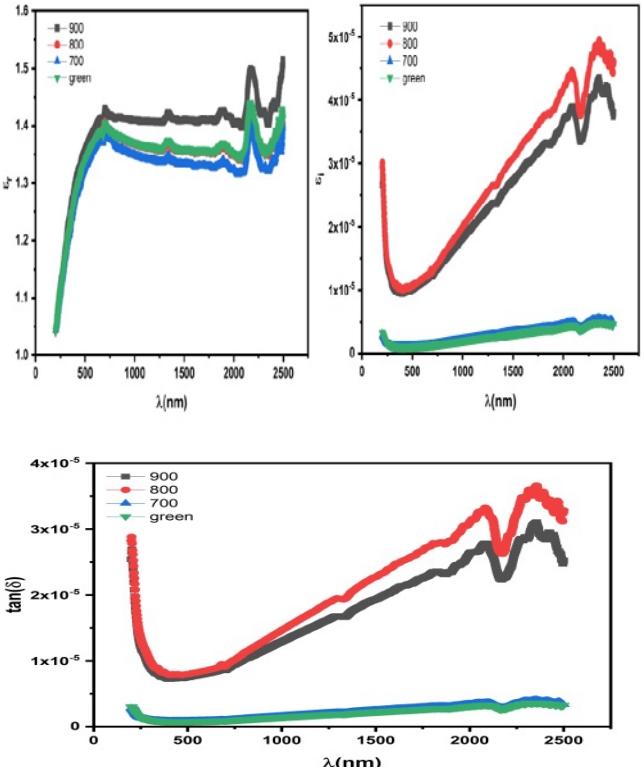

Fig. 3 The real and imaginary parts of the dielectric constant as well as tan(δ) dependency for the samples on wavelength.

When examining the electronic states of materials, optical conductivity is a crucial property [17]. The variation in optical conductivity with wavelength is displayed in Fig. 4. After a first decline in optical conductivity, the steady state is reached at (σ=1.47×108), or λ=550 nm. However, a change in the annealing temperature has no effect on the optical conductivity. The samples' decreased conductivity as wavelength increases suggests a decrease in the mobility and/or concentration of the free carriers [18].

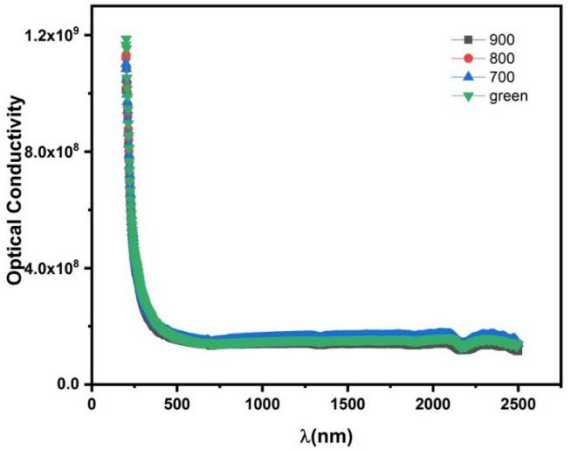

Fig. 4 wavelength dependency on the optical conductivity for the Unheated and annealed samples (T_{an}= 700, 800, 900°C)

Conclusion:

Optical and dielectric properties of as prepared and annealed NCMO were studied. The samples impedance exhibited characteristics of a capacitor's dielectric material. The AC conductivity tends to be semimetal with increasing the annealing temperatures. The somewhat high values of E_g results make these sample a candidate to be used as an absorber in the solar cell system applications. The peculiarity happening in some results of the sample annealed at 800^oC makes it used in many applications in the dielectric and optical field

References

1. Jonker, G. H., and J. H. Van Santen. "Ferromagnetic compounds of manganese with perovskite structure." *physica* 16.3 (1950): 337-349.
2. Vanitha, P. V., et al. "Effect of substitution of Mn3+ by Ni3+ and Co3+ on the charge-ordered states of the rare earth manganates, Ln0. 5A0. 5MnO3." *Solid state communications* 109.3 (1998): 135-140.
3. Rao, C. N. R., et al. "Charge ordering in the rare earth manganates: the experimental situation." *Journal of Physics: Condensed Matter* 12.7 (2000): R83.
4. Ahmed, A. M., et al. "Thermopower and magnetocaloric properties in NdSrMnO/CrO3 composites." *Journal of Magnetism and Magnetic Materials* 456 (2018): 217-222.
5. Rao, S. S., et al. "Weakening of charge order and antiferromagnetic to ferromagnetic switch over in Pr0. 5Ca0. 5MnO3 nanowires." *Applied Physics Letters* 87.18 (2005).
6. Rao, S. S., et al. "Suppression of charge order, disappearance of anti-ferromagnetism, and emergence of ferromagnetism in Nd 0.5 Ca 0.5 MnO 3 nanoparticles." *Physical Review B—Condensed Matter and Materials Physics* 74.14 (2006): 144416.
7. Anuradha, K. N., S. S. Rao, and S. V. Bhat. "Complete' melting' of charge order in hydrothermally grown Pr0. 57Ca0. 41Ba0. 02MnO3 nanowires." *Journal of nanoscience and nanotechnology* 7.6 (2007): 1775-1778.
8. Anuradha, K. N., P. R. Koushalya, and S. V. Bhat. "Size dependent magnetic properties of Nd0. 7Ca0. 3MnO3 nanomanganite." *IOP Conference Series: Materials Science and Engineering*. Vol. 73. No. 1. IOP Publishing, 2015.
9. Sanchez, R. D., et al. "Giant magnetoresistance in fine particle of La0. 67Ca0. 33MnO3 synthesized at low temperatures." *Applied Physics Letters* 68.1 (1996): 134-136.
10. Zhu, T., et al. "Surface spin-glass behavior in La2/3Sr1/3MnO3 nanoparticles." *Applied Physics Letters* 78.24 (2001): 3863-3865.
11. Troyanchuk, I. O., et al. "Phase transition in perovskites." *Journal of Physics: Condensed Matter* 10.36 (1998): 7957.
12. Mohamed, Sara, et al. "Influence of annealing temperature on structural, electrical, and magnetic properties of Nd0. 7Ca0. 3MnO3." *Electrical, and Magnetic Properties of Nd0. 7ca0. 3mno3* (2023).
13. Zhu, Jixin, et al. "Hierarchical hollow spheres composed of ultrathin Fe 2 O 3 nanosheets for lithium storage and photocatalytic water oxidation." *Energy & Environmental Science* 6.3 (2013): 987-993.
14. Alhazime, Ali A. "Effect of nano CuO doping on structural, thermal and optical properties of PVA/PEG blend." *Journal of Inorganic and Organometallic Polymers and Materials* 30.11 (2020): 4459-4467.
15. Frost, Jarvist M., et al. "Atomistic origins of high-performance in hybrid halide perovskite solar cells." *Nano letters* 14.5 (2014): 2584-2590.
16. Ezealigo, Blessing N., et al. "Method to control the optical properties: Band gap energy of mixed halide Organolead perovskites." *Arabian Journal of Chemistry* 13.1 (2020): 988-997.
17. Abd El-Raheem, M. M. "Optical properties of GeSeTl thin films." *Journal of Physics: Condensed Matter* 19.21 (2007): 216209.
18. Al-Asbahi, Bandar Ali, et al. "Effect of deposition method on the structural and optical properties of CH3NH3PbI3 perovskite thin films." *Optical Materials* 103 (2020): 109836.

Corresponding author**: Ibrahim Yousef Khaled**

Department of Basic Science, Faculty of Physiotherapy, Merit University

Email: ibrahimyousef646@gmail.com

Phone: +20 1149076788